MedChemComm

CONCISE ARTICLE

Cite this: *Med. Chem. Commun.*, 2014, **5**, 1729

Macrocyclic derivatives of 6-methyluracil as ligands of the peripheral anionic site of acetylcholinesterase†

Vyacheslav E. Semenov,*[a] Rashit Kh. Giniyatullin,[a] Sofya V. Lushchekina,[b] Ekaterina D. Kots,[c] Konstantin A. Petrov,[ade] Alexandra D. Nikitashina,[ade] Oksana A. Minnekhanova,[a] Vladimir V. Zobov,[ae] Evgeny E. Nikolsky,[adef] Patrick Masson[eg] and Vladimir S. Reznik[a]

Received 28th May 2014
Accepted 18th August 2014

DOI: 10.1039/c4md00225c

www.rsc.org/medchemcomm

Novel pyrimidinophanes possessing two *o*-nitrobenzylethyldialkylammonium heads bridging with different spacers were prepared. Pyrimidinophanes **2a**, **2b** and **3** are reversible inhibitors of cholinesterases. They show a very good selectivity for human acetylcholinesterase (AChE), with an inhibitory power 100–200 times higher than for human butyrylcholinesterase (BChE). Docking simulations indicate specific binding of pyrimidinophanes **2a** and **4** onto the peripheral anionic site of AChE. Other compounds bind to the active center of AChE as well as to the peripheral anionic site. These compounds are dual binding site inhibitors. Pyrimidinophane **2b** and its acyclic counterpart **1** were tested in the animal model of myasthenia gravis and may be considered as valuable candidates for the treatment of pathological muscle weakness syndromes.

Introduction

Acetylcholinesterase (AChE) inhibitors are widely used in medicine for pharmacological correction of cholinergic neurotransmission pathologies.[1,2] The efficacy of anti-AChE drugs is based on their ability to potentiate the effects of acetylcholine (ACh) due to a decrease in the rate of AChE-catalyzed hydrolysis of ACh. Under these conditions, extension of the lifetime of ACh molecules is able to compensate decreases in the density of functionally active cholinergic receptors in diseases such as myasthenia gravis (MG) and Alzheimer's disease.

Crystallographic studies showed that the active site of AChE is located at the bottom of a deep gorge.[3] It was shown that, in addition to its catalytic center, AChE has other sites that are crucial for the proper functioning of the enzyme. In particular, the so-called peripheral anionic site (PAS) located at the entrance of the active site gorge is responsible for: (1) allosteric modulation of the catalytic center; (2) enzyme inhibition at a high substrate concentration; (3) and non-catalytic functions such as enhancement of cell adhesion and neurite outgrowth.[4] Especially interesting is the relationship between the PAS and pathological beta-amyloid deposition. This led to a new hypothesis for the rational design of more effective anti-Alzheimer drugs.[5]

Unfortunately, the functions of the PAS of AChE have never been investigated in living organisms. At the moment all data were obtained only *in vitro* or in cell cultures because the assortment of AChE PAS ligands that can be used *in vivo* is extremely limited. Customary used PAS ligands are: (i) propidium and thioflavine (initially developed as fluorescent probes for nucleic acids and the apoptosis process); (ii) gallamine, D-tubocurarine (myorelaxants) and BW284C51 (that also blocks muscle nicotinic receptors)[6]; (iii) fasciculin-2 (a 61 amino acid peptide from the venom of the green mamba).[7] Low selectivity of these compounds for AChE *in vivo* (except fasciculin) makes their application as therapeutic agents unpromising. Fasciculin inhibits AChE in the nanomolar range. However, multiple administrations of this toxin may induce an immune response in animal models.

Several "dual binding site" inhibitors of AChE have also been described. These inhibitors bind to both active sites (usually with higher affinity).[8] To the best of our knowledge, no specific effort has yet been made to synthesize compounds for *in vivo* application that inhibit AChE by binding solely to PAS.

We described previously a new class of selective mammalian AChE *vs.* butyrylcholinesterase (BChE) inhibitors based on alkylammonium derivatives of 6-methyluracil of acyclic

[a]*A. E. Arbuzov Institute of Organic and Physical Chemistry, Arbuzov str. 8, Kazan 420088, Russia. E-mail: sve@iopc.ru; Fax: +7-843-273-18-72*
[b]*N. M. Emanuel Institute of Biochemical Physics, Moscow 119991, Russia*
[c]*M. V. Lomonosov Moscow State University, Moscow 119991, Russia*
[d]*Kazan Institute of Biochemistry and Biophysics, Kazan 420111, Russia*
[e]*Kazan Federal University, Kazan 420000, Russia*
[f]*Kazan State Medical University, Kazan 420012, Russia*
[g]*DYNAMOP, Institut de Biologie Structurale, Grenoble 38000, France*

† Electronic supplementary information (ESI) available: Synthesis procedures, analytical data and pharmacological methods. See DOI: 10.1039/c4md00225c

topology, in a particular compound (**1**, Fig. 1).[9] Compound **1** and other 1,3-bis[5-(diethyl-*o*-substitutedbenzyl)pentyl)]-5(6)-substituted uracil derivatives showed a very high affinity for AChE. In the present study, taking compound **1** as a model AChE inhibitor, we attempted to develop AChE inhibitors that specifically bind to the PAS with weak binding to the active site of AChE.

In particular, herein, in continuation of research on new AChE inhibitors among alkylammonium derivatives of 5(6)-substituted uracil derivatives, we synthesized the macrocyclic counterparts of compound **1**, pyrimidinophanes (**2a,b**, **3**, and **4**, Fig. 1), and investigated them as AChE and BChE inhibitors. Pyrimidinophanes are macrocycles consisting of pyrimidine, and in particular uracil moieties bridged to each other with alkyl spacers.[10] These macrocycles exhibit several biological activities,[10] and it is worth noting their inhibitory action towards enzymes.[11]

Pyrimidinophanes (**2a,b**, **3**, and **4**) contain the same structural moiety as acyclic compound **1**, namely 1,3-bis[5-(*o*-nitrobenzylethylammonium)pentyl]-6-methyluracilic unit. These macrocycles can be considered as macrocyclic counterparts of acyclic compound **1**. It is supposed that restriction in flexibility of the alkylammonium moieties compared to acyclic compound **1** can provide specific binding to AChE, in particular to its PAS. In addition, the alkylammonium moiety can change the type of inhibition of AChE. In our opinion, cyclization of compound **1** makes the ligand too bulky to reach the catalytic center of AChE. In order to elucidate structure–activity relationships, the onium groups in pyrimidinophanes were bridged with various spacers.

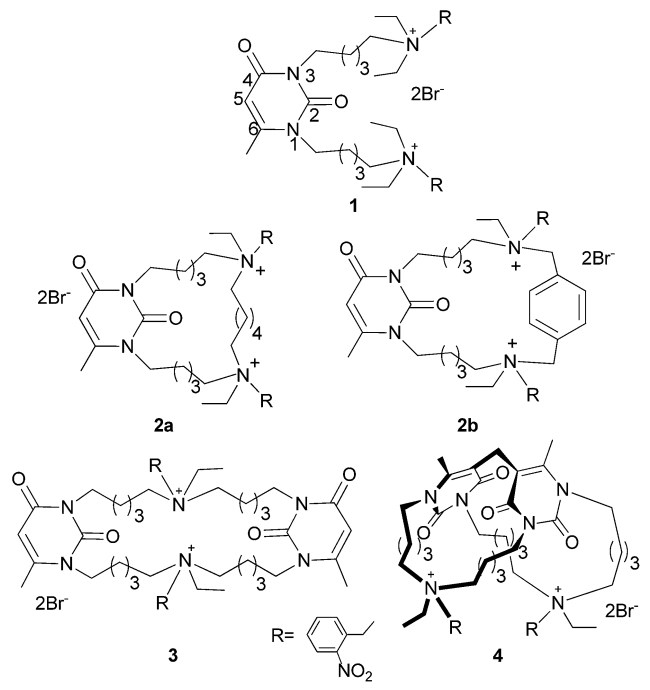

Fig. 1 Structures of acyclic and macrocyclic AChE inhibitors containing the 1,3-bis[5-(*o*-nitrobenzylethylammonium)pentyl-6-methyluracilic moiety. In compound **1**, the atom numeration in the uracil ring is shown.

Especially in pyrimidinophanes (**2a** and **2b**), the fragment was cyclized by hexamethylene and *p*-xylylene spacers, respectively, while in pyrimidinophanes (**3** and **4**) the 1,3-bis(5-pentyl)-6-methyluracil moiety was used for cyclization of the onium units. Moreover, in macrocycle **4**, an additional methylene bridge was introduced between uracil rings to increase the conformational rigidity of the compound. It is believed that the specific binding of these acyclic and macrocyclic alkylammonium 6-methyluracil derivatives to AChE is tuned by altering (i) topology acyclic or macrocyclic compounds, and (ii) rigidity of the spacers.

Results and discussion

Chemistry

The pyrimidinophanes (**2a,b**, **3**, and **4**) were synthesized starting from dibromide **5** and diamine **6**, the latter was obtained from **5** and ethylamine. This step was described elsewhere.[12] Cyclization of the diamine **6** with 1,6-dibromohexane and *p*-xylylene dibromide led to pyrimidinophanes (**7a,b**), respectively. Water-soluble pyrimidinophanes (**2a,b**) were prepared by quaternization of the nitrogen atom in bridges of macrocycles **7a,b** with *o*-nitrobenzyl bromide **8** (Scheme 1). Pyrimidinophanes (**2a** and **2b**) have 2 chiral centers, and the 4 stereoisomers of each macrocycle can occur. The individual stereoisomers were not isolated, the racemic mixtures of the macrocyclic stereoisomers were used in biological assays.

Interaction of dibromide **5** with diamine **6** resulted in a mixture of geometric *trans*- and *cis*-isomers, one of them, *cis*-isomer **9**, reacting with *o*-nitrobenzyl bromide **8** gave pyrimidinophane (**3**).[12] The intramolecular methylene bridge between C^5 of the uracil rings of pyrimidinophane (**9**) was introduced by a ring-closure reaction of the macrocycle with paraformaldehyde in aqueous 1.0 M HCl at 140 °C. The product of this reaction, a cryptand-like pyrimidinophane (**10**), was isolated. Recently, we prepared a series of pyrimidinophanes with intra- and intermolecular methylene spacers, using this approach.[13] The last step in Scheme 2 led to the aimed pyrimidinophane **4**.

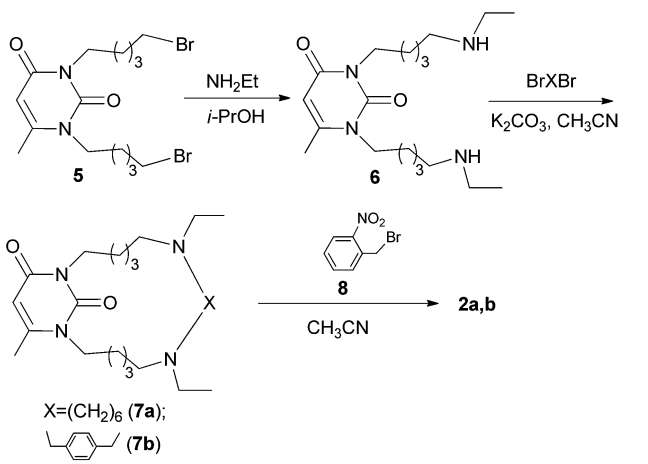

Scheme 1 Synthesis of macrocyclic AChE inhibitors with one 6-methyluracil moiety.

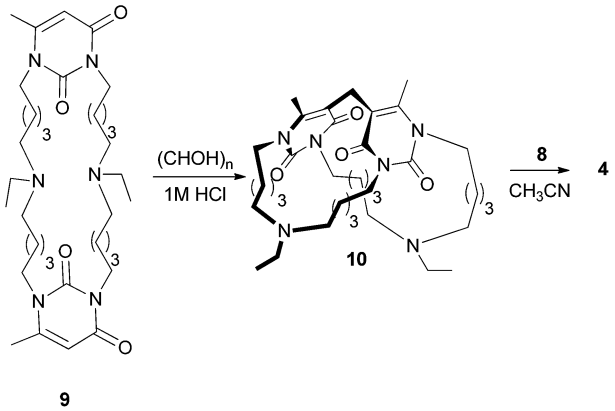

Scheme 2 Synthesis of cryptand-like macrocyclic AChE inhibitor.

Pharmacology

The inhibition potency, expressed as IC_{50}, of acyclic and macrocyclic alkylammonium derivatives of 6-methyluracil against AChE and BChE is shown in Table 1.

Acyclic compound **1** previously synthesized by our group[9] was used as the scaffold for the synthesis of macrocyclic derivatives. It was shown that cyclization of compound **1** into pyrimidinophanes (**2a,b**, **3** and **4**) resulted in decreasing anti-AChE potency. In particular, introduction of the additive uracil moiety (pyrimidinophane (**3**)) and subsequent bridging of both uracil units *via* a methylene spacer (pyrimidinophane (**4**)) markedly diminished the strength of AChE inhibition compared to compound **1**. Pyrimidinophane **2a** with a hexamethylene spacer showed a decrease in selectivity for AChE *vs.* BChE compared to compound **1**. Insertion of the phenyl moiety within the bridge binding nitrogen atoms (pyrimidinophane (**2b**)) slightly improved the inhibitory power towards AChE, thereby increasing the selectivity for AChE *vs.* BChE. It should be noted that the affinity of pyrimidinophanes **2a,b** for AChE is in the nanomolar range whereas the difference in inhibition preference for AChE *vs.* BChE is of several orders.

The mechanism of AChE inhibition was investigated using acyclic compound **1** and the most active macrocyclic compound, pyrimidinophane (**2b**). Two concentrations of each inhibitor were chosen. For each inhibitor concentration, the initial velocity (V) of substrate hydrolysis was measured at different substrate (S) concentrations ranging from 0.05 to 1 mM. The Lineweaver–Burk (L–B) plot, *i.e.* the reciprocal of the initial velocity ($1/V$) *versus* the reciprocal of the substrate concentration ($1/S$) was built (Fig. 2 and 3). The plot showed that inhibition was non-competitive. The secondary replot of the L–B slope *versus* the inhibitor concentration (Fig. 2, inset) provided a good estimate of the inhibition constants, $K_I = 0.08 \pm 0.005$ nM for compound **1** and $K_I = 50.12 \pm 1.41$ nM for pyrimidinophane **2b**. The K_I value for pyrimidinophane **2b** is higher than IC_{50} (Table 1). Cheng and Prusoff described the relationships between IC_{50} and K_I.[14] The fact that $K_I > IC_{50}$ indicates that inhibition is of mixed type with K_{Ic} higher than K_{Inc}. This situation is described by eqn (1) (see Experimental section). Since experiments were performed at $[S] \gg K_M$ ($[S] = 2$ mM, $K_M = 0.13$ mM), eqn (1) becomes eqn (2) with $\alpha = K_{Ic}/K_{Inc} > 1$. Calculation gave an estimation of $\alpha = 6.4$. This indicates that pyrimidinophane **2b** binds preferentially to the ES complex, and inhibits formation of products as a non-competitive inhibitor, *i.e.* $K_I \approx K_{Inc}$.

Because all studied compounds contain quaternary nitrogen atoms in their structure that impair penetration across the blood–brain barrier, these compounds are of potential interest for treatment of myasthenic syndromes but not for treatment of CNS pathologies.

The potential interest for *in vivo* applications of the most powerful inhibitors compound **1** and pyrimidinophane **2b** was tested for their ability to abolish symptoms of muscle weakness in an experimental autoimmune model of myasthenia gravis (EAMG). After EAMG diagnosis, compound **1**, pyrimidinophane **2b**, pyridostigmine bromide or an equivalent volume of water was injected intraperitonealy (IP) to rats. The doses of compound **1** and pyrimidinophane **2b** restoring the value of integral muscle action potential (AP) decrement in animals with EAMG to the level of healthy animals were selected. The dose of compound **1** was 0.008 mg kg^{-1}, IP (Table 2). This dose is 125 times less than LD_{50} of compound **1** in rats (1 mg kg^{-1}, IP). The dose of pyrimidinophane **2b** which restored the level of

Table 1 *In vitro* inhibition of AChE from human erythrocytes and human plasma BChE by pyrimidinophanes **2a,b**, **3** and **4** compared to pyridostigmine bromide[a,b]

	IC_{50} [nM]		
Compd	AChE	BChE	AChE selectivity[c]
1	0.14 ± 0.068	10 000 ± 12 458.0	66 667
2a	59 ± 7.67	9200 ± 1137.4	156
2b	7.0 ± 0.085	1200 ± 175.4	171
3	130 ± 19.5	10 000 ± 1124.5	77
4	4000 ± 523.0	20 000 ± 2463.6	5
Pyridostigmine bromide	350 ± 19.6	1000 ± 142.6	3

[a] Values are expressed as mean ± standard error of three independent measurements. The concentration range for the tested compounds was from 10^{-10} to 10^{-5} M (10 concentration points with increments of about a half). [b] Acetylthiocholine and butyrylthiocholine concentration was 2 mM. [c] (IC_{50} BChE)/(IC_{50} AChE).

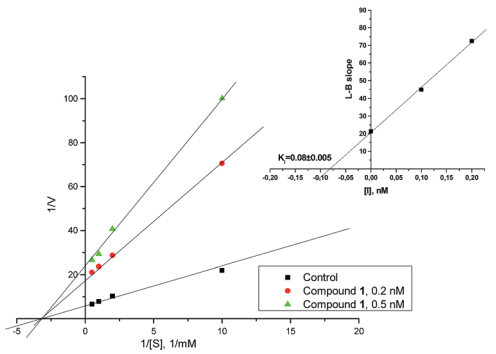

Fig. 2 Reversible inhibition of AChE by compound **1** under steady-state conditions. A double reciprocal plot of initial velocity *vs.* substrate concentration in the absence of inhibitor and at two inhibitor concentrations. Inset: a secondary replot of L–B plot *versus* inhibitor concentration.

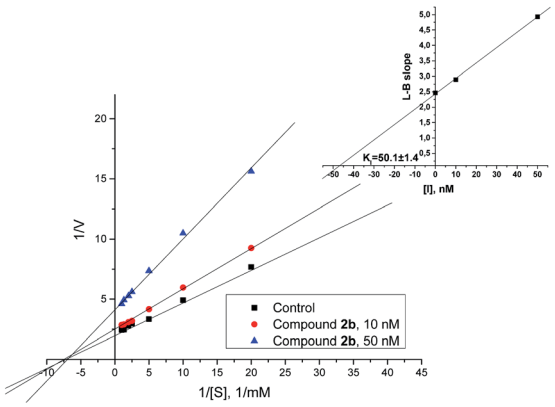

Fig. 3 Reversible inhibition of AChE by pyrimidinophane **2b** under steady-state conditions. A double reciprocal plot of initial velocity *vs.* substrate concentration in the absence of an inhibitor and at two inhibitor concentrations. Inset: secondary replot of L–B plot *versus* inhibitor concentration.

decrement up to control was 0.3 mg kg^{-1} in IP administration (Table 2), which is 50 times lower than LD_{50} of pyrimidinophane **2b** for rats (15.5 mg kg^{-1}, IP). A similar effect in the EAMG model was achieved by pyridostigmine injection, 0.1 mg kg^{-1} (Table 2). This dose is only 27 times lower than LD_{50} of pyridostigmine for rats (2.7 mg kg^{-1}, IP). In addition to its toxicity, comparable or lower than that of pyridostigmine, compound **1** and pyrimidinophane **2b** have another advantage for myasthenia gravis treatment. Compound **1** and pyrimidinophane **2b** are more selective for AChE *vs.* BChE than pyridostigmine (Table 1). The use of specific (AChE) or non-specific (AChE and BChE) inhibitors to treat myasthenia was previously discussed.[15] BChE is abundant in human plasma (the average concentration is 50 nM) and present in many cells and organs but its inhibition cannot improve muscle contraction of patients with myasthenia. Clinical studies have indicated that inhibition of plasma BChE may result in potentiating peripheral side effects.[16] Moreover, the activity level of BChE is variable in human population due to large genetic polymorphism,[17] and to physiological status. So that doses of BChE inhibitors needed for different patients are different. Thus, non-specific covalent inhibitors, such as pyridostigmine, are more difficult to use because they bind and react first with plasma BChE whose concentration level and reactivity may vary between individuals. The plasma BChE issue does not affect the action of specific AChE inhibitors, especially the action of compound **1** or pyrimidinophane **2b**. Thus, compound **1** and pyrimidinophane **2b** can be considered as a valuable therapeutical candidate for the treatment of pathological muscle weakness syndromes.

Molecular modeling

In order to explain the different inhibitory properties of compound **1** and its macrocyclic counterparts, pyrimidinophanes, and to clarify their interaction mode in the active center gorge of AChE, molecular docking studies were performed using the X-ray structure 2HA2 [18] of murine AChE with succinyldicholine and its half-hydrolyzed product in the active site gorge. This structure solved at 2.05 Å, is the best one among all murine AChE X-ray structures available in the PDB.[19] In addition, the presence of a bifunctional substrate molecule in the gorge makes this structure most suitable for docking of bulky ligands. Due to the high number of torsion degrees of freedom in compound **1**, docking parameters were adjusted in series of test runs with succinyldicholine, which displays 11 possible torsions. The selected parameters assured that the docked position of succinyldicholine corresponded with the X-ray data.

The most favorable binding energies estimated from molecular docking simulations are provided in Table 3. The binding energy can be converted into an inhibition constant using standard equation[20] $\Delta G_{bind} = RT \ln K_I$, where the gas

Table 2 Decrement of muscle AP amplitude in the control group (healthy animals) and in animals with EAMG

	Ratio of 1st to 200th AP amplitudes (decrement) %	
Compound, dose, mg kg^{-1}	Healthy animals	EAMG animals
Water	95.00 ± 1.00	67.3 ± 2.7
2b, 0.1 mg kg^{-1}	—	75.0 ± 1.8
2b, 0.3 mg kg^{-1}	—	95.4 ± 1.0
1, 0.004 mg kg^{-1}		83.25 ± 1.38
1, 0.008 mg kg^{-1}		95.41 ± 0.96
Pyridostigmine bromide, 0.1 mg kg^{-1}	—	91.3 ± 1.9

Table 3 Binding energy to AChE gorge calculated from molecular docking

Compd	1	2a	2b	3	4
ΔG_{bind}, kcal mol^{-1}	−13.72	−9.45	−10.81	−7.73	−7.36

constant $R = 1.987$ cal K^{-1} mol^{-1}, and the absolute temperature $T = 310$ K because K_I was determined experimentally at 37 °C. For linear compound **1** this gives a docking K_I value of 0.212 nM. This calculated value is in good agreement with the experimental value. Indeed, converting experimental K_I value into the binding free energy at 310 K we obtain −14.32 kcal mol^{-1}. This value differs only by 0.6 kcal mol^{-1} from the calculated value −13.72 kcal mol^{-1}.

Compound **1** occupies the whole gorge of AChE from the active site to the PAS. In the active site the nitro group of one of the nitrobenzene ring forms hydrogen bonds both with the catalytic serine and oxyanion hole (Gly121 and Gly122), while its phenyl ring is parallel to the phenyl ring of Phe338 which ensures strong π–π interaction between them. The adjacent tetraalkylammonium group is surrounded by aromatic rings of Trp86 and Tyr337, establishing strong π-cation interactions with them. There is a hydrogen bond between the hydroxyl-group of Tyr124 and oxygen of the 6-methyluracyl ring, while the ring itself is parallel to Tyr342 and has strong π–π interaction with it. The second tetraalkylammonium group is not far from Trp286, however positioning of its indole ring is not favorable for π-cation interactions. Rather it shows a good hydrophobic contact with the linker chain between the 6-methyluracil ring and the ammonium group. The nitro group of the second nitrophenyl ring establishes hydrogen bonds with the side chain and the peptide group of Ser293 of the PAS (Fig. 4).

Due to the induced fit step, molecular dynamics (MD) simulation of the protein-inhibitor complex final adjustment[21] improved positioning of compound **1** inside the AChE gorge. 30 ns MD trajectory revealed the following adjustments in the complex structure (Fig. 5): the tetraalkylammonium group located at the bottom of the gorge and the adjacent nitrobenzene ring moved further down the gorge. Then, the tetraalkylammonium group formed new strong electrostatic interaction

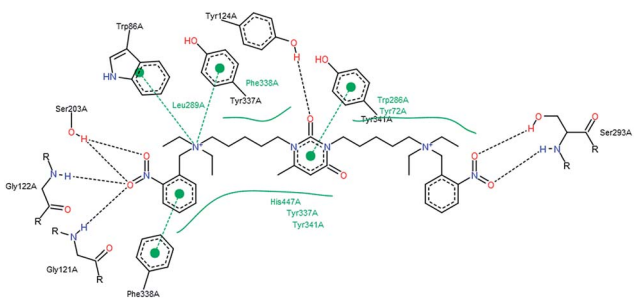

Fig. 4 2D scheme of the position of compound **1** docked inside AChE active site gorge, showing main interactions with amino acid residues. Image generated using PoseView software.

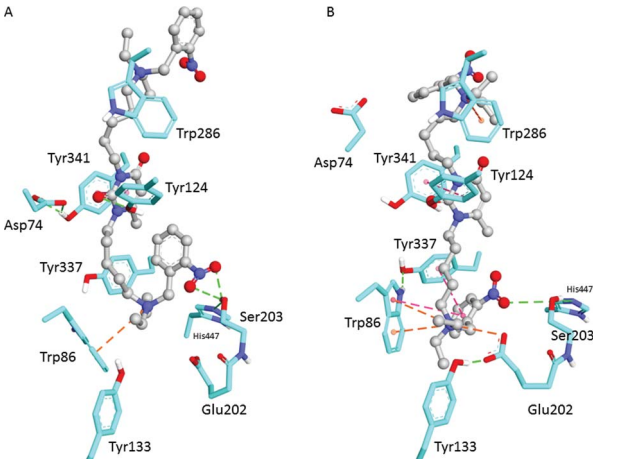

Fig. 5 Position of the compound **1** inside AChE gorge according to (A) molecular docking study with rigid protein and (B) after MD simulation. Carbon atoms of the inhibitor and AChE gorge are shown in grey and cyan, respectively.

with Glu202, whose carboxylate position moved to fulfill this interaction. As a result, it is interesting to point out that Glu202 formed a hydrogen bond with Tyr133. π-Cation interaction of the tetraalkylammonium head with Trp86 was retained, while π-cation interaction with Tyr337 was lost due to displacement of the tetraalkylammonium group further down the gorge. Instead, the nitrobenzene ring became in a favorable position to interact with Tyr337. Though the nitrobenzene ring had moved 6 Å down the gorge, orientation of the nitro group was still occupying the active center, in immediate proximity of the catalytic Ser203. In the final complex structure, because the 6-methyluracil ring position did not change at all, it can be concluded that pushing down the tetraalkylammonium and nitrobenzene groups resulted from stretching of the linker chain. Tyr124 and Tyr341 moved close to the 6-methyluracil ring for a tighter interaction. An important structural change is the displacement of Asp74, which in the X-ray structure forms hydrogen bond with Tyr341. After MD simulation, Asp74 is found to be turned away from Tyr341. This allows the second tetraalkylammonium group and the nitrobenzene ring to move deeper into the PAS and to interact with its components more tightly. Now, compared to the position obtained by docking into the rigid protein, the tetraalkylammonium group is facing the indole ring of Trp286, establishing a strong π-cation interaction.

Macrocyclic counterparts of compound **1** display considerably lower affinity for AChE. Pyrimidinophanes (**2a** and **2b**) have 2 chiral centers, thus the 4 stereoisomers of each compound were considered. For pyrimidinophanes (**2a,b**) the lowest binding energy among all stereoisomers was provided, in both cases this was (*R*,*R*)-enantiomer; for **2a** difference in binding energies of all stereoisomers was within 1 kcal mol^{-1}, and 1.5 kcal mol^{-1} for **2b**. The binding energy calculated for compound **2b** after conversion into an inhibition constant gives $K_I = 23.9$ nM. This value is also in good agreement with experimental data. The experimental binding free energy, −10.35 kcal mol^{-1},

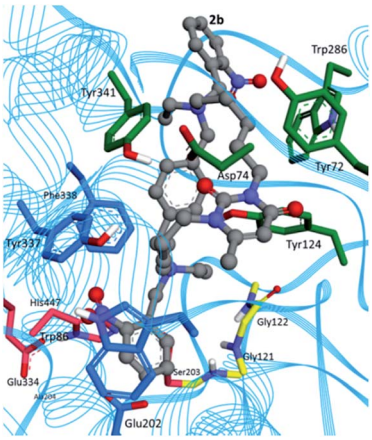

Fig. 6 Molecular docking study on pyrimidinophane **2b** (carbon atoms are grey). Catalytic triad residues (Ser203, His447 and Glu334) are shown in red, catalytic binding sub-site residues (Trp86, Glu202, Tyr337, and Phe338) are shown in blue, oxyanion hole residues (Gly121, Gly122 and Ala204) are shown in yellow, and peripheral anionic site residues (Tyr72, Asp74, Tyr124, Trp286, and Tyr341) are shown in green.

differs from the calculated one by less than 0.5 kcal mol^{-1}. The calculated binding energies for other compounds correlate well with measured IC_{50} values.

The most favorable docked position for the (*R*,*R*)-enantiomer of the pyrimidinophane **2b** was deeply inside the gorge, one nitrophenyl ring forming π–π interactions with Trp86 at the bottom of the gorge, and a quaternary ammonium group forming π-cation interactions with Phe338 and Tyr337, while the other part of the compound occupied the PAS area (Fig. 6).

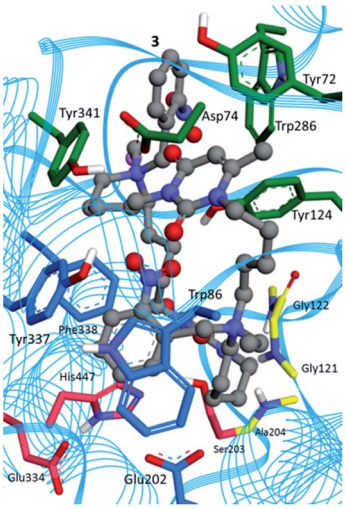

Fig. 7 Molecular docking study on pyrimidinophane **3** (carbon atoms are grey). Catalytic triad residues (Ser203, His447 and Glu334) are shown in red, catalytic binding sub-site residues (Trp86, Glu202, Tyr337, and Phe338) are shown in blue, oxyanion hole residues (Gly121, Gly122 and Ala204) are shown in yellow, and peripheral anionic site residues (Tyr72, Asp74, Tyr124, Trp286, and Tyr341) are shown in green.

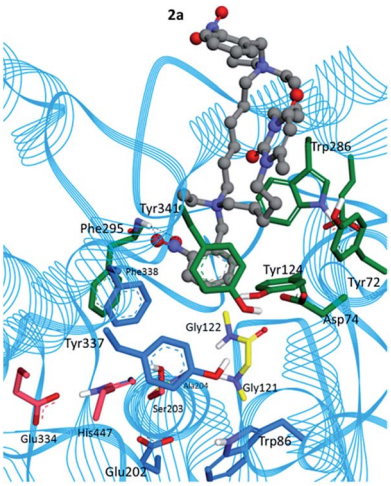

Fig. 8 Molecular docking study on pyrimidinophane **2a** (carbon atoms are grey). Catalytic triad residues (Ser203, His447 and Glu334) are shown in red, catalytic binding sub-site residues (Trp86, Glu202, Tyr337, and Phe338) are shown in blue, oxyanion hole residues (Gly121, Gly122 and Ala204) are shown in yellow, and peripheral anionic site residues (Tyr72, Asp74, Tyr124, Trp286, and Tyr341) are shown in green.

The other stereoisomers show similar binding energies but were located in PAS and did not reach the gorge bottom.

Pyrimidinophane **3** occupies the whole gorge from PAS to the active site, in the catalytic anionic sub-site, the nitrophenyl ring is parallel to the Trp86 indole ring, that ensures good π–π-interactions; the nitro group forms hydrogen bonds with the Tyr337 phenolic hydroxyl group; one quaternary ammonium

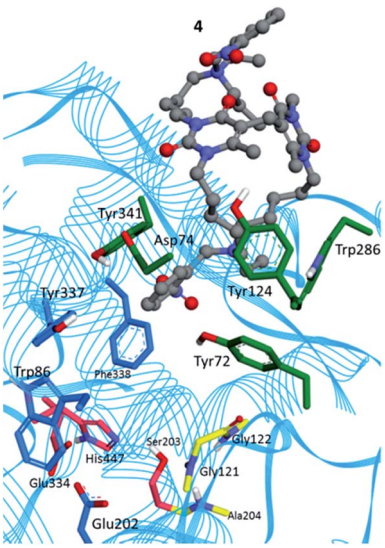

Fig. 9 Molecular docking study on pyrimidinophane **4** (carbon atoms are grey). Catalytic triad residues (Ser203, His447 and Glu334) are shown in red, catalytic binding sub-site residues (Trp86, Glu202, Tyr337, and Phe338) are shown in blue, oxyanion hole residues (Gly121, Gly122 and Ala204) are shown in yellow, and peripheral anionic site residues (Tyr72, Asp74, Tyr124, Trp286, and Tyr341) are shown in green.

group interacts with Asp74. However, the positively charged quaternary ammonium group is located in the oxyanion hole, what is rather unfavorable (Fig. 7).

For pyrimidinophanes (**2a** and **4**), no position deeply buried in the gorge with good binding energies was found. Instead, in the best docked positions, the macrocycles **2a** ((*R*,*R*)-enantiomer) and **4** occupy PAS (Fig. 8 and 9). Both molecules show the same specific interactions with PAS amino acids: one nitrophenyl ring has π–π interactions with Tyr341, its nitro group forms hydrogen bonds with Phe295 backbone nitrogen, and the quaternary ammonium group is located favorably for π-cation interactions with the Trp286 ring. However, due to the more rigid macrocyclic structure, pyrimidinophane **4** binds to PAS weaker than macrocycle **2a**.

Conclusions

In this study we attempted to increase the size of AChE ligands to restrict specific binding to the PAS of AChE. To this aim we synthesized new pyrimidinophanes bearing two *o*-nitrobenzylethyldialkylammonium heads. Almost all of synthesized pyrimidinophanes inhibited AChE in the nanomolar range. Based on molecular docking simulations, it was suggested that compounds **1**, **2b**, and **3** bind AChE to the active center as well as to the PAS. Compounds **2a** and **4** bind preferentially with PAS. Thus, we found that introduction of the spacer, flexible or rigid, between [5-(*o*-nitrobenzylethylammonium)pentyl] units at N atoms of the 6-methyluracil moiety allows tuning the binding of 6-methyluracil derivatives with AChE. In conclusion, it can be stated that pyrimidinophanes **2a** and **4** are promising lead scaffold structures for further design of specific ligands for the PAS of AChE. Also AChE inhibitors with a 6-methyluracil moiety may be considered as potential drugs for the treatment of pathological muscle weakness syndromes.

Acknowledgements

This work was supported by RFBR grant 13-00-40286 K and by the subsidy of the Russian Government to support the Program of Competitive Growth of Kazan Federal University among World's Leading Academic Centers. The authors wish to thank Dr Al-Shekhadat (Biomedical Center, St. Petersburg, Russia) for synthesis of peptide for induction of EAMG.

Notes and references

1 T. Brenner, E. Nizri, M. Irony-Tur-Sinai, Y. Hamra-Amitay and I. Wirguin, *J. Neuroimmunol.*, 2008, **201–202**, 121–127.
2 J. L. Cummings, *Am. J. Psychiatry*, 2000, **157**, 4–15.
3 H. Dvir, I. Silman, M. Harel, T. L. Rosenberry and J. L. Sussman, *Chem.-Biol. Interact.*, 2010, **187**, 10–22.
4 L. E. Paraoanu and P. G. Layer, *FEBS J.*, 2008, **275**, 618–624.
5 M. Singh, M. Kaur, H. Kukreja, R. Chugh, O. Silakari and D. Singh, *Eur. J. Med. Chem.*, 2013, **70**, 165–188.
6 S. Olivera-Bravo, I. Ivorra and A. Morales, *Br. J. Pharmacol.*, 2005, **144**, 88–97.
7 E. Karlsson, P. M. Mbugua and D. Rodriguez-Ithurralde, *Am. J. Physiol.*, 1984, **79**, 232–240.
8 D. Genest, C. Rochais, C. Lecoutey, J. Sopkova-de Oliveira Santos, C. Ballandonne, S. Butt-Gueulle, R. Legay, M. Since and P. Dallemagne, *MedChemComm*, 2013, **4**, 925–931.
9 K. A. Anikienko, E. A. Bychikhin, V. S. Reznik, V. D. Akamsin and I. V. Galyametdinova, *Chem.-Biol. Interact.*, 2008, **175**, 286–292.
10 V. E. Semenov, *J. Inclusion Phenom. Macrocyclic Chem.*, 2013, **77**, 1–22.
11 U. Luecking, G. Siemeister, M. Schaefer, H. Briem, M. Krueger, P. Lienau and P. Jautela, *ChemMedChem*, 2007, **2**, 63–77.
12 V. E. Semenov, A. D. Voloshina, E. M. Toroptzova, N. V. Kulik, V. V. Zobov, R. K. Giniyatullin, A. S. Mikhailov, A. E. Nikolaev, V. D. Akamsin and V. S. Reznik, *Eur. J. Med. Chem.*, 2006, **41**, 1093–1101.
13 V. E. Semenov, R. K. Giniyatullin, A. S. Mikhailov, A. E. Nikolaev, S. V. Kharlamov, S. K. Latypov and V. S. Reznik, *Eur. J. Org. Chem.*, 2011, **28**, 5423–5426.
14 Y. Cheng and W. H. Prusoff, *Biochem. Pharmacol.*, 1973, **22**, 3099–3108.
15 M. Komloova, K. Musilek, M. Dolezal, F. Gunn-Moore and K. Kuca, *Curr. Med. Chem.*, 2010, **17**, 1810–1824.
16 E. C. Hulme, N. J. M. Birdsall and N. J. Buckley, *Annu. Rev. Pharmacol. Toxicol.*, 1990, **30**, 633–673.
17 B. Benyamin, R. P. Middelberg, P. A. Lind, A. M. Valle, S. Gordon, D. R. Nyholt, S. E. Medland, A. K. Henders, A. C. Heath, P. A. F. Madden, P. M. Visscher, D. T. O'Connor, G. W. Montgomery, N. G. Martin and J. B. Whitfield, *Hum. Mol. Genet.*, 2011, **20**, 4504–4514.
18 Y. Bourne, Z. Radic, G. Sulzenbacher, E. Kim, P. Taylor and P. Marchot, *J. Biol. Chem.*, 2006, **281**, 29256–29267.
19 H. M. Berman, J. Westbrook, Z. Feng, G. Gilliland, T. N. Bhat, H. Weissig, I. N. Shindyalov and P. E. Bourne, *Nucleic Acids Res.*, 2000, **28**, 235–242.
20 G. M. Morris, D. S. Goodsell, R. S. Halliday, R. Huey, W. E. Hart, R. K. Belew and A. J. Olson, *J. Am. Chem. Soc.*, 1998, **19**, 1639–1662.
21 S. V. Lushchekina, E. D. Kots, P. Masson, K. A. Petrov and E. E. Nikolsky, *Slow, tight-binding inhibition of acetylcholinesterase by alkylammonium derivatives of 6-methyluracil: a molecular dynamics study* is currently under preparation, methodology and results will be detailed in this work.